ORGANIC
LETTERS

2002
Vol. 4, No. 13
2185−2188

Hydrogen-Bonded Charge-Transfer Complexes of TTF Containing a Uracil Moiety: Crystal Structures and Electronic Properties of the Hydrogen Cyananilate and TCNQ Complexes

Yasushi Morita,*,† Suguru Maki,† Makoto Ohmoto,† Hiroshi Kitagawa,‡,§
Takashi Okubo,§ Tadaoki Mitani,§ and Kazuhiro Nakasuji*,†

Department of Chemistry, Graduate School of Science, Osaka University, Toyonaka, Osaka 560-0043, Japan, Department of Chemistry, University of Tsukuba, Tsukuba, Ibaraki 305-8571, Japan, and Japan Advanced Institute of Science & Technology, Tatsunokuchi, Ishikawa 923-1292, Japan

morita@chem.sci.osaka-u.ac.jp

Received April 18, 2002

ABSTRACT

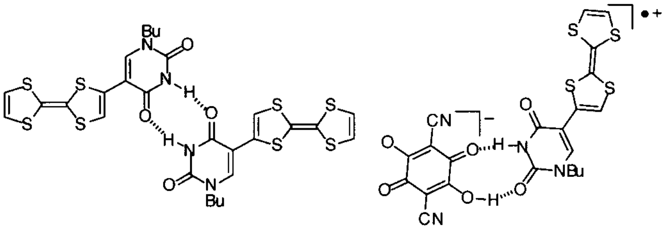

A novel TTF-based donor with a uracil moiety, TTF-(1-*n*-butyluracil-5-yl) (T*n*bU), was synthesized. Crystal structures of both T*n*bU and the charge-transfer complex of T*n*bU–hydrogen cyananilate possess complementary double hydrogen bonds through uracil moieties and π-stacking dimer structures between TTF skeletons. Furthermore, the T*n*bU–TCNQ charge-transfer complex shows a high electrical conductivity underlying the partial charge-transfer accompanied by a hydrogen-bonding interaction, which was substantiated in terms of the measurements of the IR, electronic spectra, and conductivity.

Noncovalent bonds such as the $\pi\cdots\pi$ interaction and hydrogen-bonding (H-bonding) play a fundamentally important role in a wide range of phenomena from the conductivity of organic based materials to sequence-specific DNA recognition.[1] The $\pi\cdots\pi$ interaction for tetrathiafulvalene (TTF) derivatives crucially affects electronic conduction behavior, and numerous organic (super)conductors were synthesized.[2] By using specific H-bonding to control the conducting column structures, solid-state assemblies, and molecular recognition, TTF derivatives with hydroxyl,[3a,b] carboxyl,[3c,d] thioamido,[3e−h] and pyrrole[3i,j] groups and a directly uracil-fused TTF system[4] have been designed and prepared. The effective interplay between charge-transfer (CT) and H-bonding interactions on the molecular assemblies is currently appreciated as an important concept and method in the construction of new molecular materials and fine-tuning of their physical properties, which was first observed in quinhydrone systems.[5] A variety of H-bonded CT complexes can be candidates to realize such cooperative proton−

[†] Osaka University.
[‡] University of Tsukuba.
[§] Japan Advanced Institute of Science & Technology.

(1) (a) For recent overview of H-bonding, see: *The Weak Hydrogen Bond*; Desiraju, G. R., Steiner, T., Eds.; Oxford University Press: New York, 1999; Chapter 1.

(2) *Organic Superconductors*, 2nd ed.; Ishiguro, T., Yamaji, K., Saito, G., Eds.; Springer-Velrag: Berlin; Tokyo, 1998.

10.1021/ol020081z CCC: $22.00

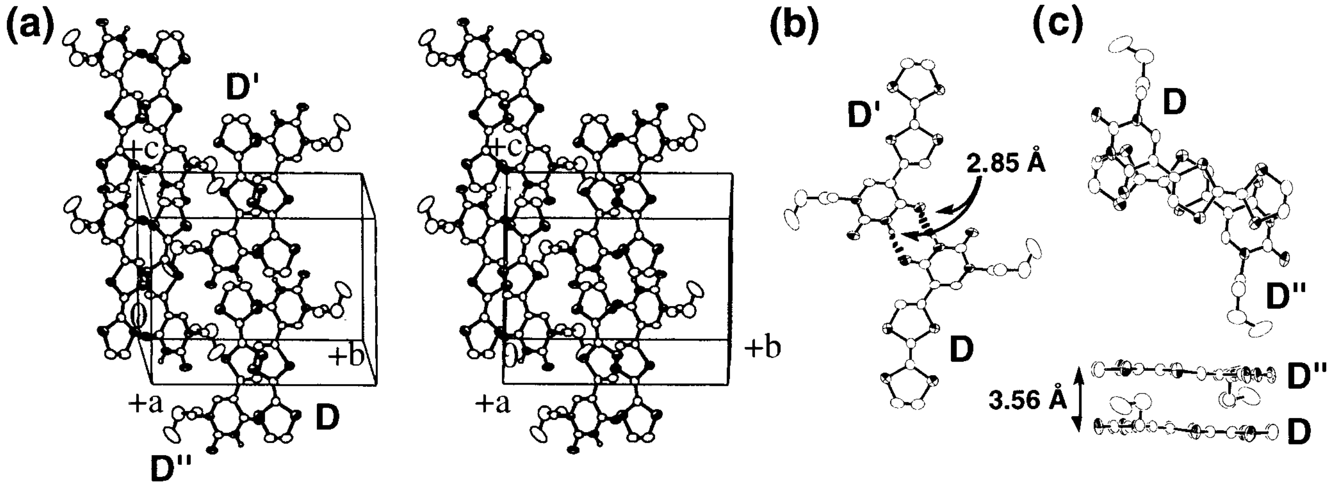

Figure 1. Crystal structure of T*n*bU. **D**, **D′**, and **D″** denote T*n*bU molecules. Stereoview of crystal packing (a), complementary H-bonding of dimer (b). The closest $C^4{=}O\cdots H{-}N^3$ contacts are shown by dotted lines. The overlap mode of π-stacking dimer (c).

electron systems.[6] The recent theoretical studies for the model polymers containing DNA base pairs and a successful synthesis of the TTF derivative with a uracil moiety, TU, have encouraged us to explore the CT complexes of TU-based molecules with electron acceptors.[7] In this Letter, we deal with the synthesis of *n*-butyl-substituted TU, T*n*bU, and its CT complexes with 2,5-dicyano-3,6-dihydroxy-1,4-benzoquinone (cyananilic acid, H_2CNAL)[6e−h] and TCNQ. The H-bonding architecture constructed by uracil moieties and $HCNAL^-$ as well as the electronic properties of the CT complexes are demonstrated in terms of X-ray crystal structure analysis, IR, and electronic spectra.

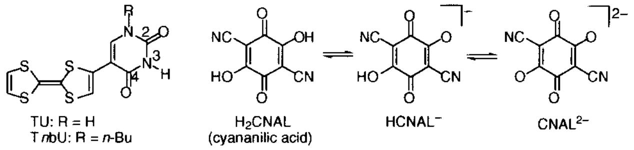

T*n*bU was prepared by the Stille cross-coupling reaction of the tributylstannyl-substituted TTF derivative[7c] with 1-*n*-butyl-5-iodouracil[8] in the presence of $Pd(PPh_3)_4$ in toluene.[9] The cyclic voltammogram of T*n*bU in DMF shows two-stage, one-electron reversible oxidation waves.[10] Interestingly, the slightly negative shift of two oxidation potentials of T*n*bU compared with those of TTF was observed (T*n*bU: E_1, −0.102; E_2, +0.095. TTF: E_1, −0.080; E_2, +0.116), indicating that T*n*bU has a good electron donating ability as well as a high stability of the oxidation states. A single crystal of T*n*bU suitable for X-ray structure analysis was obtained by the vapor diffusion method using hexane−THF.[11] T*n*bU crystallizes in the monoclinic space group $P2_1/c$ and forms the π-stacking dimers which are connected by the complementary double hydrogen bonds between uracil moieties to make a one-dimensional arrangement along the *c*-axis (Figure 1). The closest O···N contacts within an

---

(3) (a) Blanchard, P.; Boubekeur, K.; Sallé, M.; Duguay, G.; Jubault, M.; Gorgues, A.; Martin, J. D.; Canadell, E.; Auban-Senzier, P.; Jérome, D.; Batail, P. *Adv. Mater*. **1992**, *4*, 579−581. (b) Dolbecq, A.; Fourmigué, M.; Batail, P. *Chem. Mater*. **1994**, *6*, 1413−1418. (c) Dolbecq, A.; Fourmigué, M.; Batail, P. *Bull. Soc. Chim. Fr*. **1996**, *133*, 83−88. (d) Kepert, C. J.; Hesek, D.; Beer, P. D.; Rosseinsky, M. J. *Angew. Chem., Int. Ed*. **1998**, *37*, 3158−3160. (e) Batsanov, A. S.; Bryce, M. R.; Cooke, G.; Dhindsa, A. S.; Heaton, J. N.; Howard, J. A. K.; Moore, A. J.; Petty, M. C. *Chem. Mater*. **1994**, *6*, 1419−1425. (f) Moore, A. J.; Bryce, M. R.; Batsanov, A. S.; Heaton, J. N.; Lehmann, C. W.; Howard, J. A. K.; Robertson, N.; Underhill, A. E.; Perepichka, I. F. *J. Mater. Chem*. **1998**, *8*, 1541−1550. (g) Heuzé, K.; Fourmigué, M.; Batail, P. *J. Mater. Chem*. **1999**, *9*, 2373−2379. (h) Ono, G.; Izuoka, A.; Sugawara, T. Sugawara, Y. *J. Mater. Chem*. **1998**, *8*, 1703−1709. (i) Chen, W.; Cava, M. P.; Takassi, M. A.; Metzger, R. M. *J. Am. Chem. Soc*. **1988**, *110*, 7903−7904. (j) Zong, K. Chen, W.; Cava, M. P.; Rogers, R. D. *J. Org. Chem*. **1996**, *61*, 8117−8124.

(4) (a) Neiland, O. Y.; Tilika, V. Z.; Edzhinya, A. S. *Chem. Heterocycl. Comp*. **1992**, 945−950. (b) Neilands, O.; Belyakov, S.; Tilika, V.; Edzina, A. *J. Chem. Soc., Chem. Commun*. **1995**, 325−326. (c) Neilands, O.; Tilika, V.; Sudmale, I.; Grigorjeva, I.; Edzina, A.; Fonavs, E.; Muzikante, I. *Adv. Mater. Opt. Electron*. **1997**, *7*, 93−97. (d) Neilands, O.; Liepinsh, V.; Turovska, B. *Org. Lett*. **1999**, *1*, 2065−2067.

(5) (a) Nakasuji, K.; Sugiura, K.; Kitagawa, T.; Toyoda, J.; Okamoto, H.; Okaniwa, K.; Mitani, T.; Yamamoto, H.; Murata, I.; Kawamoto, A.; Tanaka, J. *J. Am. Chem. Soc*. **1991**, *113*, 1862−1864. (b) Mitani, T.; Inabe, T. In *Spectroscopy of New Materials*; Clark, R. J. H., Hester, R. E., Eds.; John Wiley & Sons Ltd.: 1993; Chapter 6.

(6) (a) Sugiura, K.; Toyoda, J.; Okamoto, H.; Okaniwa, K.; Mitani, T.; Kawamoto, A.; Tanaka, J.; Nakasuji, K. *Angew. Chem., Int. Ed. Engl*. **1992**, *31*, 852−854. (b) Kitagawa, H.; Mitani, T.; Itoh, T.; Toyoda, J.; Nakasuji, K. *Synth. Met*. **1995**, *71*, 1919−1920. (c) Yoshida, D.; Kitagawa, H.; Mitani, T.; Itoh, T.; Nakasuji, K. *Synth. Met*. **1997**, *86*, 2105−2106. (d) Tamaki, K.; Morita, Y.; Toyoda, J.; Yamochi, H.; Saito, G.; Nakasuji, K. *Tetrahedron Lett*. **1997**, *38*, 4583−4586. (e) Zaman, Md. B.; Morita, Y.; Toyoda, J.; Yamochi, H.; Saito, G.; Yoneyama, N.; Enoki, T.; Nakasuji, K. *Chem. Lett*. **1997**, 729−730. (f) Zaman, Md. B.; Toyoda, J.; Morita, Y.; Nakamura. S.; Yamochi, H.; Saito, G.; Nakasuji, K. *Synth. Met*. **1999**, *102*, 1691−1692. (g) Yamochi, H.; Nakamura, S.; Saito, G.; Zaman, Md. B.; Toyoda, J.; Morita, Y.; Nakasuji, K.; Yamashita, Y. *Synth. Met*. **1999**, *102*, 1729. (h) Zaman, Md. B.; Toyoda, J.; Morita, Y.; Nakamura, S.; Yamochi, H.; Saito, G.; Nishimura, K.; Yoneyama, N.; Enoki, T.; Nakasuji, K. *J. Mater. Chem*. **2001**, *11*, 2211−2215.

(7) (a) Shigeta, Y.; Nagao, H.; Toyoda, J.; Morita, Y.; Nakasuji, K.; Yoshioka, Y.; Yamaguchi, K. *Int. J. Quantum Chem*. **2000**, *80*, 882−891. (b) Shigeta, Y.; Nagao, H.; Yoshioka, Y.; Toyoda, J.; Morita, Y.; Nakasuji, K.; Yamaguchi, K. *Synth. Met*. **2001**, *119*, 259−260. (c) Maki, S.; Morita, Y.; Kitagawa, S.; Mitani, T.; Nakasuji, K. *Synth. Met*. **2001**, *120*, 741−742.

H-bonding dimer is 2.85 Å (Figure 1b). The face-to-face distance between the π-stacking TTF planes is 3.56 Å (Figure 1c). In a solution IR spectra (ClCH$_2$CH$_2$Cl, 1×10^{-3} M, Figure 2a), T*n*bU shows absorption bands at 1716 and 1693 cm^{-1}, which can be assigned to $C^2{=}O$ and $C^4{=}O$ stretching vibrations, respectively, by the experimental and theoretical studies of uracil derivatives.[12] In the solid state, the absorption band of the $C^4{=}O$ stretching frequency at 1693 cm^{-1} shifts to a significantly lower frequency (1655 cm^{-1}) due to the complementary H-bonding ($C^4{=}O \cdots H{-}N^3$) (Figure 2b).

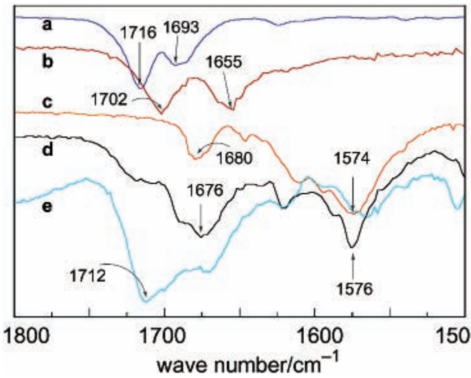

Figure 2. IR spectra of T*n*bU (ClCH$_2$CH$_2$Cl solution, a; KBr pellet, b), Bu$_4$N$^+$·HCNAL$^-$ (KBr pellet, c),[15] T*n*bU$^{\bullet+}$·HCNAL$^-$ complex (KBr pellet, d), and TnbU-TCNQ complex (KBr pellet, e).

The CT complexes of T*n*bU with HCNAL$^-$ and TCNQ were obtained. Diffusion of an ethyl acetate−CH$_3$CN (1:1) solution of T*n*bU and H$_2$CNAL in an H-tube gave single crystals of the T*n*bU$^{\bullet+}$·HCNAL$^-$ complex as green plates.[13] In the crystal structure, the unit cell is composed of **D**, **A**, and CH$_3$CN in a 1:1:1 ratio (Figure 3).[11] The complementary H-bonding between T*n*bU$^{\bullet+}$ and HCNAL$^-$ is constructed through $C^2{=}O \cdots H{-}O$ (2.58 Å) and $N^3{-}H \cdots O{=}C$ (2.84 Å) (Figures 3a and 3e). The H-bonding influences the $C^2{=}O$ stretching to shift to a lower frequency (1676 cm^{-1}) (Figure 2d).[14] The formation of the complementary H-bonding found in the complex represents the first example among the H$_2$-CNAL-based CT complexes in which all of the hydrogen bonds are between the HCNAL$^-$ molecules themselves.[6e−h] In addition, T*n*bU$^{\bullet+}$ forms specific C−H···X type hydrogen bonds with two HCNAL$^-$'s (X represents oxygen and nitrogen atoms of HCNAL$^-$, Figure 3e). The stacking structure of this complex has two types: (i) **AD** type alternated stacking along the *c*-axis and (ii) **ADDA** type stacking along the [011] direction with 3.46 for **DD** and 3.40 Å for **AD** (Figure 3b). In the head-to-tail mode overlap of **DD**, S···S contact is observed (3.36−3.46 Å). The intense absorption band at 12 000 cm^{-1} was assigned to the intermolecular CT transition between the radical cation moieties of T*n*bUs (Figure 4c).[16] The electronic spectrum and the nitrile stretching frequency at 2208 cm^{-1} provide a rationale for a complete ionic complex, giving rise to complex being an insulator (Table 1).

Table 1. Physical Properties of HCNAL$^-$ or TCNQ Complex

CT complexes	CN stretching, cm^{-1}	ionicity	CT band, cm^{-1}	conductivity σ_{rt}, S cm^{-1}
T*n*bU$^{\bullet+}$·HCNAL$^-$	2208	1[a]	12000	$<10^{-8}$
T*n*bU−TCNQ	2196	0.7[b]	3000	0.07
TU−TCNQ[c]	2196	0.7[b]	3000	0.11

[a] The CN stretching frequencies of neutral H$_2$CNAL·6H$_2$O and Bu$_4$N$^+$·HCNAL$^-$ were 2236 and 2206 cm^{-1}, respectively.[15] [b] The ionicity of TCNQ was estimated by the CN stretching frequency of the IR spectrum on the basis of the Chappell method.[19] [c] See ref 7c.

CT complex of T*n*bU and TCNQ was prepared as a black green microcrystalline solid by mixing an ethyl acetate solution of each compound; molar ratio was estimated to be 1:0.7 by elemental analysis.[17] In the IR spectrum, the carbonyl stretching frequency was observed at 1712 cm^{-1}, which is similar to that of T*n*bU in solution (Figures 2a and 2e). Furthermore, in the nitrile stretching region (2210−2160 cm^{-1}), the lower frequency band near 2167 cm^{-1} (B_{2u} mode) became active and broadened remarkably with decreasing temperature.[6b,c,7c,18] Thus, we infer the formation of a weak H-bonding interaction such as the $CN \cdots H{-}N^3$ type in the T*n*bU−TCNQ complex, although the possibility of $C{=}O \cdots H{-}N$ type H-bonding may not be excluded. The ionicity of TCNQ was estimated to be 0.7 in terms of the

---

(8) (a) Israel, M.; Zoll, E. C.; Muhammad, N.; Modest, E. J. *J. Med. Chem.* **1973**, *16*, 1−5. (b) Naim, A.; Shevlin, P. B. *Synth. Commun.* **1990**, *20*, 3439−3440. (c) Robins, M. J.; Barr, P. J.; Giziewicz, J. *Can. J. Chem.* **1982**, *60*, 554−557.

(9) Mp 221−223 °C (dec); TLC R_f 0.58 (1:1 hexane/ethyl acetate); ^{1}H NMR (270 MHz, DMSO-d_6) δ 0.90 (t, 3, J = 7.3 Hz), 1.26 (m, 2), 1.57 (m, 2), 3.74 (t, 2, J = 7.3 Hz), 6.74 (s, 2), 7.36 (s, 1), 7.81 (s, 1), 11.64 (brs, 1); IR (KBr) 3400, 3033, 2956, 1702, 1655 cm^{-1}; EI-MS, *m/z* 370 (M$^+$, 79%). Anal. Calcd for C$_{14}$H$_{14}$N$_2$O$_2$S$_4$: C, 45.38; H, 3.81; N, 7.56. Found: C, 45.79; H, 3.83; N, 7.33.

(10) Cyclic voltammograms were carried out using the following conditions: 5 mM in DMF with 0.1 M Bu$_4$N$^+$ClO$_4^-$ as supporting electrolyte at room temperature versus a Ag/Ag$^+$ reference electrode at a sweep rate of 100 mV/s. The final results were calibrated with the ferrocene/ferrocenium couple; see also Supporting Information.

(11) A detailed result for X-ray analysis is shown in the CIF file. See Supporting Information.

(12) (a) Nyquist, R. A.; Fiedler, S. L. *Vib. Spectrosc.* **1995**, *8*, 365−386. (b) Portalone, G.; Bencivenni, L.; Colapietro, M.; Pieretti, A.; Ramondo, F. *Acta Chim. Scand.* **1999**, *53*, 57−68, and references therein.

(13) Mp 197−199 °C (dec); IR (KBr) 3600−3300, 3190, 3100−2700, 2208, 1676, 1576 cm^{-1}; UV (KBr) 280, 386, 608, 822, 852 nm. Anal. Calcd for (C$_{14}$H$_{14}$N$_2$O$_2$S$_4$)(C$_8$HO$_4$)(CH$_3$CN): C, 47.99; H, 3.02; N, 11.66. Found: C, 47.84; H, 3.06; N, 11.38.

(14) The carbonyl stretching frequency of the HCNAL$^-$ moiety (1576 cm^{-1}) was not strongly influenced by the intermolecular H-bonding with T*n*bU$^{\bullet+}$ compared with that of Bu$_4$N$^+$·HCNAL$^-$ (Figures 2c and 2d).[15]

(15) Preparation of Bu$_4$N$^+$·HCNAL$^-$ will be reported elsewhere.

(16) Torrance, J. B.; Scott, B. A.; Welber, B.; Kaufman, F. B.; Seiden, P. E. *Phys. Rev.* **1979**, *B19*, 730−741.

(17) Mp 209−210 °C (dec); IR (KBr) 2196, 2181, 1712 cm^{-1}; UV (KBr) 380, 630, 854, 2096, 2364, 2402, 2516 nm. Anal. Calcd for (C$_{14}$H$_{14}$N$_2$O$_2$S$_4$)-(C$_{12}$H$_4$N$_4$)$_{0.7}$: C, 52.40; H, 3.30; N, 13.09. Found: C, 52.06; H, 3.19; N, 13.12.

(18) The temperature dependence of the IR spectra (nitrile stretching range) of the T*n*bU−TCNQ complex is shown in the Supporting Information.

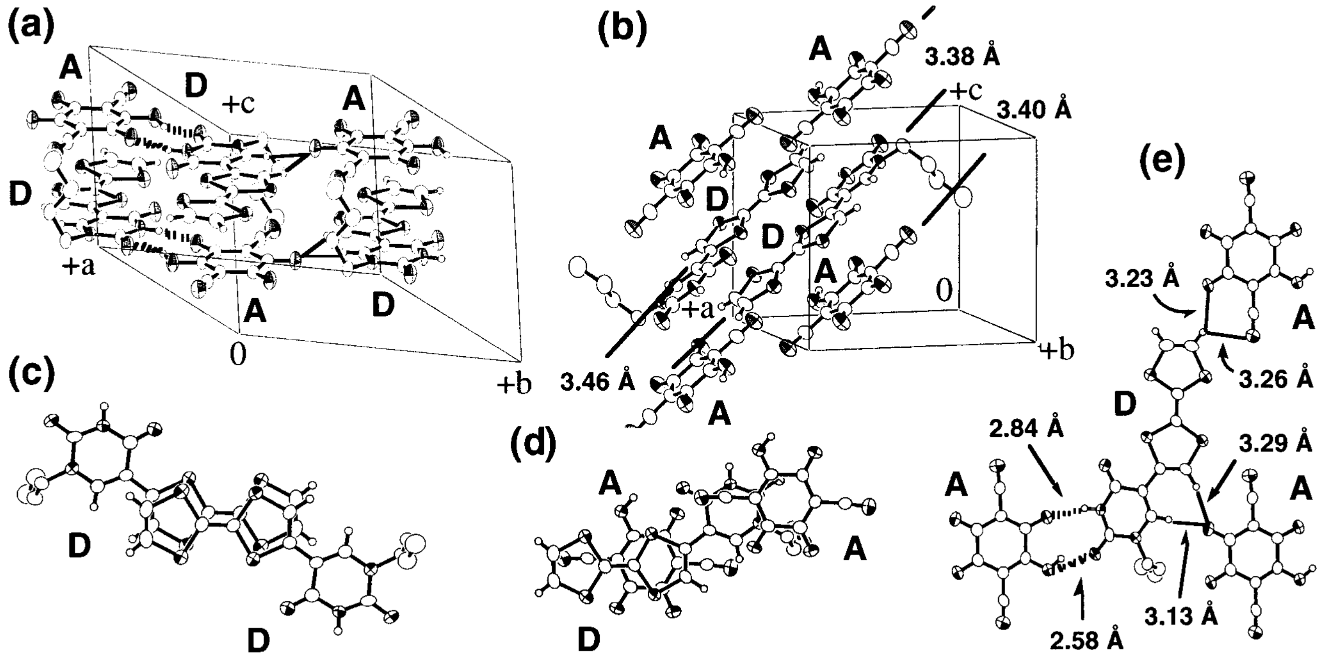

Figure 3. Crystal structure of T*n*bU$^{\bullet+}$·HCNAL$^-$ CT complex. **D** and **A** denote T*n*bU$^{\bullet+}$ and HCNAL$^-$ molecules, respectively. CH$_3$CN molecules are omitted for clarity. The shortest C^2=O···H–O (O–O length, 2.58 Å) and N^3–H···O=C (N–O length, 2.84 Å) contacts are shown by dotted lines. Solid lines show C–H···X H-bonding where X represents O and N atoms (the cited length indicates C–X length). H-bonded interaction along the *b*-axis (a), stacking diagram of **ADDA** and **AD** stacks (b), overlap pattern in **ADDA** stack and in **AD** stack, respectively (c and d), intermolecular bond lengths between **A** and **D** on the same plane (e).

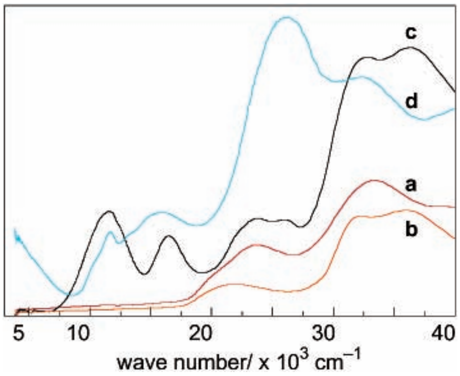

Figure 4. Electronic spectra of T*n*bU (a), Bu$_4$N$^+$·HCNAL$^-$ (b), ^{15}T*n*bU$^{\bullet+}$·HCNAL$^-$ complex (c), and T*n*bU–TCNQ complex (d) in KBr pellet.

nitrile stretching frequency of the B_{1u} mode (2196 cm^{-1}).[19] This consideration is consistent with the result from a very low-energy absorption band around 3000 cm^{-1},[20] which can be assigned to an intrastack CT transition in the TCNQ column with a partial ionicity (Figure 4d and Table 1).[16,21] Room-temperature conductivity on a compressed pellet using the four-probe method is evaluated to be 0.07 S cm^{-1} with semiconducting behavior, which is similar to that of TU–TCNQ.[7c] These two CT complexes demonstrate 10–10^4 orders higher conductivity than those of other CT complexes based on TTF derivatives having a variety of H-bonding functionalities (Table 1).[3]

In summary, we have synthesized a new electron donor molecule, T*n*bU, and its CT complexes containing an H-bonding network and substantiated that introduction of a uracil moiety provides a useful and interesting strategy for the construction of H-bonded CT complexes. For the extension of this strategy, the combination of TTF moieties and other nucleic acid bases should give not only a unique opportunity to study the interplay between proton and electron transfers but also synthetic challenges for the creation of conducting polymers based on biomolecules.

Acknowledgment. This work was supported by a Grant-in-Aid for Scientific Research on Priority Area “Delocalized π-Electronic Systems” (No. 297) from the Ministry of Education, Culture, Sports, Science and Technology, Japan and by JSPS Research Fellowships for Young Scientists (S.M.).

Supporting Information Available: Detailed experimental procedure, IR spectra, resistivity data, and crystallographic information file (CIF) for T*n*bU and T*n*bU$^{\bullet+}$·HCNAL$^-$ complex. This material is available free of charge via the Internet at http://pubs.acs.org.

OL020081Z

---

(19) Chappell, J. S.; Bloch, A. N.; Bryden, W. A.; Maxfield, M.; Poehler, T. O.; Cowan, D. O. *J. Am. Chem. Soc.* **1981**, *103*, 2442–2443.

(20) IR spectrum of this CT complex is shown in the Supporting Information.

(21) Nakasuji, K.; Nakatsuka, M.; Yamochi, H.; Murata, I.; Harada, S.; Kasai, N.; Yamamura, K.; Tanaka, J.; Saito, G.; Enoki, T.; Inokuchi, H. *Bull. Chem. Soc. Jpn.* **1986**, *59*, 207–214, and references therein.